Investigation of the role of feedstock properties and process conditions on the slow pyrolysis of biomass in a continuous auger reactor

Filipe Rego, Huan Xiang, Yang Yang, Jorge López Ordovás, Katie Chong, Jiawei Wang*, Anthony Bridgwater

Bioenergy Research Group, EBRI, Aston University, Aston Triangle, Birmingham, B4 7ET, United Kingdom

**Corresponding author: j.wang23@aston.ac.uk*

Abstract

Slow pyrolysis is a complex process that can convert biomass and waste into valuable products. An improved understanding of the influence of process conditions and feedstocks is required to inform process design and optimisation. A continuous auger reactor (300 g/h) was used to process wheat straw under slow pyrolysis conditions, to study the influence of pyrolysis temperature (400, 500, 600 °C) and solid residence time (3, 6, 10 min) on the product yields and char properties. Production of char decreased with pyrolysis temperature (35.0 to 26.7 wt.%), while gas production increased (15.8 to 29.7 wt.%). The yield of liquid product achieved a maximum of 46.8 wt.% at 500 °C. Solid residence time did not affect the product yields significantly.

Increasing the pyrolysis temperature produced an increase in the calorific value of the char, mainly through an increase in carbon and fixed carbon (FC) contents and a decrease in oxygen and volatile matter (VM) content. Higher solid residence time caused a reduction in the volatile matter of the char. The surface areas from nitrogen porosimetry at 77 K were very low for all the chars tested (below 15 m^2 g^{-1}), suggesting that the pores of the char are blocked or narrowed during

operation. FTIR data showed a significant reduction in surface chemical functionalities with pyrolysis temperature, such as C-O and C=O, and the solid residence time had no significant effect. The produced chars have the potential to be used as solid fuel, as a soil amendment, or as adsorbents for aqueous phase contaminants.

Multiple linear models were developed using literature data to estimate the product yields and properties of the char, including volatile matter, fixed carbon, ash content and higher heating values. The predicted values had a good agreement with the actual values with R^2 values in the range of 0.75-0.95. Thus, the models can be used for the design and optimisation of char production by slow pyrolysis.

Keywords: wheat straw; slow pyrolysis; auger reactor; char; multiple linear regressions

1. Introduction

A need for sustainable energy and material sources is evident due to the emergence of excessive CO_2 emissions and consequent climate change. Several advanced thermochemical and biological conversion technologies, such as gasification, pyrolysis, and anaerobic digestion, are available to utilise low-value resources. With these technologies, it is possible to utilise wastes and low-value materials as feedstock to produce a range of valuable products for various applications. For example, slow pyrolysis can process biomass, including agricultural wastes such as wheat straw, to produce char, a carbon-based solid product. Char has received increased interest recently due to its potential for valuable and practical applications, for example, as biochar for soil amendment and conditioning [1], as a catalyst [2] and catalyst support [3], or as an adsorbent for contaminant removal from gaseous [4] and aqueous streams [5].

Auger (or screw) reactors operate continuously, which can be seen as an advantage to other reactor systems commonly used for slow pyrolysis, such as batch kilns and twin-retorts. The biomass feedstock is transported along the reactor using a screw, and the solid product is usually discharged by gravity into a collection vessel. Advantages of auger reactors include: flexible and reliable control of residence time by varying the screw speed; compactness, and thus the possibility of making them modular and transportable [6], allowing for installation in decentralised or remote locations where the feedstock is abundant [7]; and their flexibility towards different feedstock types, shapes and sizes [8]. Limitations of auger reactor systems are the risk of blockages inside the reactor, which can damage the equipment (possibly leading to a replacement of the screw or even the complete reactor) and the hot moving parts, which restrict the materials used for construction. They require careful design to avoid leakages and air entrance, and there are particular challenges for scale-up, mainly due to heat transfer issues [9]. Nevertheless, continuous

auger reactors can be a cost-effective way to produce chars with beneficial uses. To aid their further development and implementation, there is a need to establish correlations between process conditions and product yields and properties.

Research regarding pyrolysis in auger reactors has been performed for various materials, such as wastes (e.g. tyres [10], WEEE [11], organic fractions of MSW [12,13]), woody biomass (e.g. pine [6,14,15], beech [16]), and herbaceous biomass (e.g. corn stalk [17], rice husk [17,18], wheat straw [18], barley straw [14], switchgrass [19]). Pyrolysis temperature was found by Fassinou *et al.* [20] to be the main driver for the process yields from pinewood pyrolysis in an auger reactor. The solid residence time (SRT) and biomass flow rate did not affect the process as significantly as pyrolysis temperature, which is the main variable controlling product yields and properties [1,21].

When using an auger reactor for slow pyrolysis between 350 and 600 °C, Yu *et al.* [17] found that rice husk produced higher char yields than corn stalk, which was linked to a higher ash content in the rice husk and led to lower energy content in the rice husk chars compared to the corn stalk chars. A study of pyrolysis of pine wood chips (up to 20 mm nominal size) by Puy *et al.* [6] in an auger reactor found that the feedstock mass flow rate (3.9 to 6.9 kg h^{-1}) did not affect the product yields and quality significantly. However, the solid residence time studied at 500 °C and with 3.9 kg h^{-1} of feedstock affected the product yield significantly when relatively low values were employed (1.5 to 3 minutes). An SRT of 5 minutes resulted in similar product yields to 3 minutes of SRT. A minimum of 2 minutes of SRT was required for pyrolysis (carbonisation) reactions to be completed. This parameter was seen to influence the proximate analysis of the chars, mainly through a decrease in the volatile matter.

Manyà has underlined the need for an improved experimental understanding of the influence of feedstock-intrinsic conditions and critical process conditions (e.g. temperature and solid

residence time) on char production [1]. As far as the authors are aware, there is a lack of an in-depth assessment of the effect of multiple variables on the char yields and properties from slow pyrolysis of biomass in a continuous auger reactor. A comprehensive comparison with the literature can optimise process parameters, and the main factors contributing to modifying product yield and properties can be established. This research has explored the suitability of using an auger reactor system for slow pyrolysis, studying how different process conditions affect the product yields and properties, focusing on the char product, using statistical analysis. The slow pyrolysis of wheat straw was analysed by varying the pyrolysis temperature and solid residence time. The relationship between the product yields, properties of char and process conditions were quantified by multiple linear regressions. The findings from this research can support scale up and optimise the slow pyrolysis of biomass for the char production in a commercial scale.

2. Materials and Methods

2.1. Characterisation of feedstock and products

An agricultural company in Belgium provided the wheat straw feedstock. The feedstock is mainly in the form of broken pellets, with dimensions ranging from small pieces of less than 0.5 cm and broken pellets of up to 1.6 cm in length and 0.8 cm in diameter. No binder was used in feedstock production. The wheat straw pellets were used as received in the slow pyrolysis experiments. The feedstock was milled and sieved to particle sizes under 0.5 cm and further milled with a coffee grinder for all physicochemical analyses.

The proximate analysis was performed with a thermogravimetric analyser (TGA/DSC2 STARe System, Mettler Toledo), based on the ASTM method E1131-08 [22]. Under nitrogen flow (30 ml min^{-1}), samples were heated up to 900 °C with a heating rate of 10 °C min^{-1}. Under oxygen flow (20 ml min^{-1}), samples were heated up to 575 °C at 10 °C min^{-1}. Ultimate analysis of the

wheat straw feedstock was performed using an organic elemental analyser (CHNS/O Flash 2000, Thermo Fisher Scientific). The results from the ultimate analysis were used to determine the higher heating value (HHV), using the Channiwala and Parikh correlation for solid fuels [23]. The characterisation of the wheat straw feedstock in terms of proximate and ultimate analyses (averaged from triplicate analyses) and the calculated higher heating value can be seen in Table 1.

Table 1. Proximate and ultimate analyses and the calculated higher heating value of the wheat straw feedstock.

Proximate analysis (wt.%, dry basis)	
Moisture [a)]	4.8
Volatile matter	79.4
Fixed carbon [b)]	16.3
Ash	4.3
Ultimate analysis (wt.%, dry ash-free basis)	
Carbon	49.3
Hydrogen	6.7
Nitrogen	0.9
Sulphur	0.1
Oxygen [b)]	43.0
HHV (MJ kg^{-1}, dry basis)	19.2

[a)] Wet basis; [b)] by difference

For the product analyses, the chars from the pyrolysis experiments were ground with mortar and pestle and sieved to particle sizes less than 425 µm. Proximate analyses were performed in the same manner as the feedstock, except that the peak temperature under an oxygen atmosphere was 750 °C, based on ASTM D1762 [24]. Elemental composition analyses were performed by an external laboratory (Medac Ltd.), and the Channiwala and Parikh correlation for solid fuels [23] was used to calculate the HHV.

The feedstock and char pH (in H_2O) was analysed with a Sartorius PB-11 pH meter pre-calibrated with pH buffers with pH = 4, 7 and 10. The suspensions in water were prepared with 1 wt.% solid loading and stirred with a magnetic stirrer for 1 hour. Analyses were performed at least in triplicate and at a temperature of 20 °C.

Nitrogen porosimetry was performed on chars using a Quantasorb Nova 4000e porosimeter. Oven-dried samples were degassed in a vacuum at 200 °C for over 2 h. Specific surface areas were calculated with the Brunauer-Emmet-Teller (BET) theory over the range P/P^0 of 0.03–0.20 of the adsorption isotherms.

The feedstock and chars were also analysed for surface chemical functionalities using Fourier Transform Infrared (FTIR, on a Perkin Elmer FT-IR Spectrometer with PIKE Technologies GladiATR and Spectrum software). The FTIR analyses were performed under a range of wavenumber of 4000 to 400 cm^{-1}, using 16 scans and 4 cm^{-1} resolution, and in triplicate to minimise experimental errors. A selected number of char products were also analysed by Scanning Electronic Microscopy (SEM), with a JEOL 7800 series equipment.

2.2. Reactor system and experimental procedure

The reactor system used in this work was a bench-scale auger system, comprising a reactor and feeding system, a vapour condensing and liquid collection system, a solid collection vessel, and a gas meter and analyser. The reactor system has been described elsewhere in detail [17], and a representation can be seen in Fig. 1.

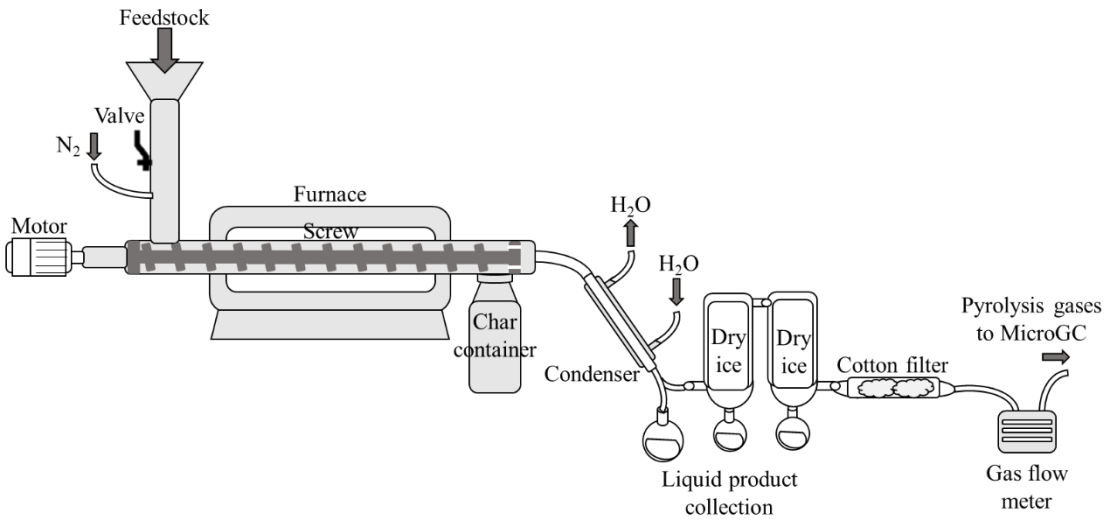

Fig. 1. Representation of the auger reactor system used for the slow pyrolysis experiments with wheat straw pellets.

Before starting the experiments, the system was purged with nitrogen (2 L min^{-1}) to establish an inert atmosphere. The water used for the condenser was at 5 °C. During operation, biomass was fed at a rate of about 5 g min^{-1} for a maximum of 1 h to obtain significant amounts of liquid and char products for post-production analyses. The employed temperatures were 400, 500 and 600°C and the solid residence times were 3, 6 and 10 minutes. The solid residence time was controlled with an electric motor that moved the screw, and the temperature inside the reactor was measured with a K-type thermocouple.

The solid and liquid products from each experiment were cooled down to room temperature before collection. Then, the solid products were removed from the char pot and stored in sealable plastic bags. The liquid products typically separated into two distinct phases by gravity, namely an organic phase and aqueous phase, and were collected separately when this occurred. All the organic phases had a lower density than the aqueous phases and hence appeared in an upper layer. The non-condensable gases were analysed by Gas Chromatography (on a Varian CP-4900 MicroGC, with 5Å Molsieve and PoraPLOT Q columns, and helium as carrier gas).

Each experiment was performed in duplicate, with average values reported, except for experiments at 500 and 600 °C with SRT of 3 minutes, because of an exchange of motor and the impossibility of employing SRT lower than 5 minutes.

2.3. Statistical analysis

To evaluate the effects of feedstock properties and process conditions on the slow pyrolysis in continuous auger reactors, experimental data was collected from literature and tabulated in Table S1 in the supplementary material. The data were analysed using the software Design Expert

12 by analysis of variance (ANOVA). In addition, multiple linear regressions were used to evaluate the relationship between the input variables (pyrolysis temperature, SRT, feedstock's volatile matter and ash content) and the responses (product yields, char's volatile matter, fixed carbon and ash content, and HHV).

3. Results and discussion

3.1. Product yields from slow pyrolysis experiments

The pyrolysis products' mass yields (dry feedstock basis) with varying pyrolysis temperature and solid residence time are listed in Table S1 and visualised in Figs. 2, 3 and 4. A closure of over 95 wt.% was obtained in all cases.

3.1.1. Char

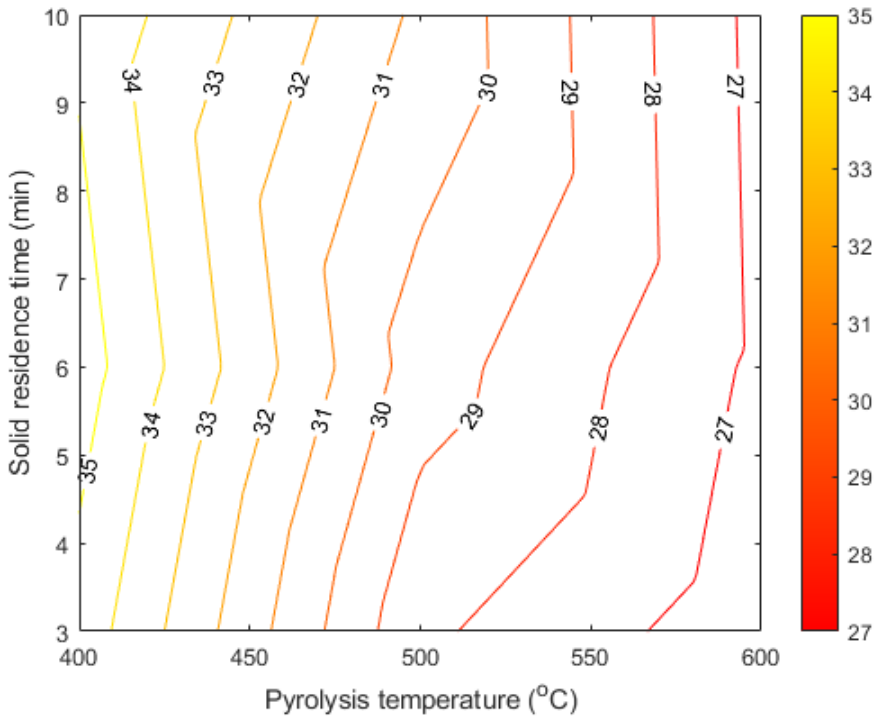

Fig. 2. Char yields (wt.%, dry basis) for the slow pyrolysis experiments with wheat straw pellets: effects of SRT and pyrolysis temperature.

As shown in Fig. 2, the contour lines of the char yield are nearly vertical, which implies that the char yield mainly depends on the pyrolysis temperature while the solid residence time has little effect on the char yield. The char yield decreased with increasing pyrolysis temperature (35.0 to 26.7 wt.%, averaged for all three SRT). Experiments by Yu *et al.* using rice husk and corn stalk in the same reactor [17] have revealed similar trends at temperatures between 350 and 600 °C. In Yu's work, char yields (dry feedstock basis) dropped from 43.9 to 31.1 wt.% for rice husk and from 33.4 to 27.0 wt.% for corn stalk. The char yields from the wheat straw feedstock were similar to corn stalk but lower than rice husk. This could be due to the differences in ash and volatile matter content (on a dry basis) in the feedstock: the rice husk had a higher ash content of 16.0 wt. % and lower volatile matter contents of 67.2%.

The solid residence time is reported in the literature to have a lesser influence on the product distribution than pyrolysis temperature, often being dominated by other factors such as temperature and heating rate [21]. Indeed, the effect of SRT on the char yields was practically negligible, indicating that carbonisation is complete at the shortest SRT of 3 minutes. For example, Puy *et al.* reported a minimum of 2 minutes for the complete devolatilization of pine wood chips at 500 °C and a feedstock flow rate of 3.9 kg h^{-1} [6]. The standard deviations of the average char yields for different SRT but the same pyrolysis temperature were 0.5, 1.3, and 0.2 wt.% (dry feedstock basis) for 400, 500, and 600 °C, respectively. This relatively small variation was considered within experimental error (the relative standard deviation is under 5 %).

3.1.2. Liquid product

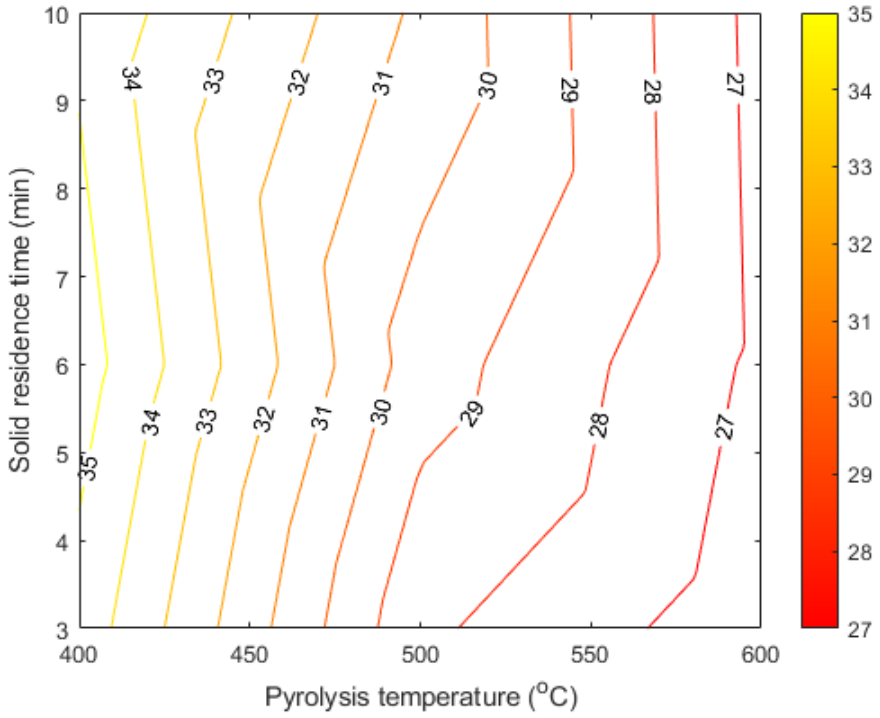

Fig. 3. Liquid yields (wt.%, dry basis) for the slow pyrolysis experiments with wheat straw pellets: effects of SRT and pyrolysis temperature.

The liquid product yields have an upside-down V-shape in the contour map (Fig. 3). Liquid product yield with the wheat straw feedstock had a maximum (about 46.8 ± 2.8 wt.%) at a temperature of 500 °C. The literature has recognised that the maximum liquid product yield is achieved at biomass pyrolysis temperatures around 500 °C [8]. In terms of aqueous and organic fractions of the pyrolysis liquid, the proportion of the aqueous phase decreased with temperature (39.3 to 33.1 wt.%), while the organic phase increased (5.7 to 9.3 wt.%). This trend can be connected to the fact that more of the lignocellulosic structure in the biomass is decomposed with temperature and contributes to the organic liquid phase, especially lignin, when temperatures are over 400 °C. Furthermore, reforming reactions are promoted at temperatures above 450 °C, reducing the yield of reaction water and thus aqueous phase [25]. This was contrary to what was

observed for wood waste pyrolysis in a lab-scale auger reactor by Solar *et al.*, which can be due to the higher temperatures employed in that work (750 and 900 °C) [15].

3.1.3. Gas products

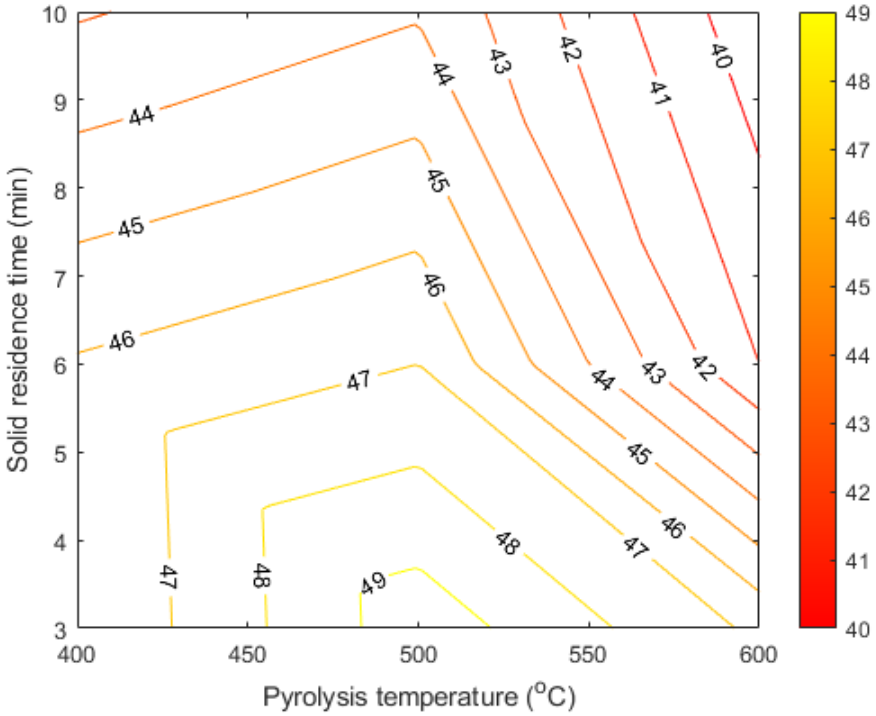

Fig. 4. Gas yields (wt.%, dry basis) for the slow pyrolysis experiments with wheat straw pellets: effects of SRT and pyrolysis temperature.

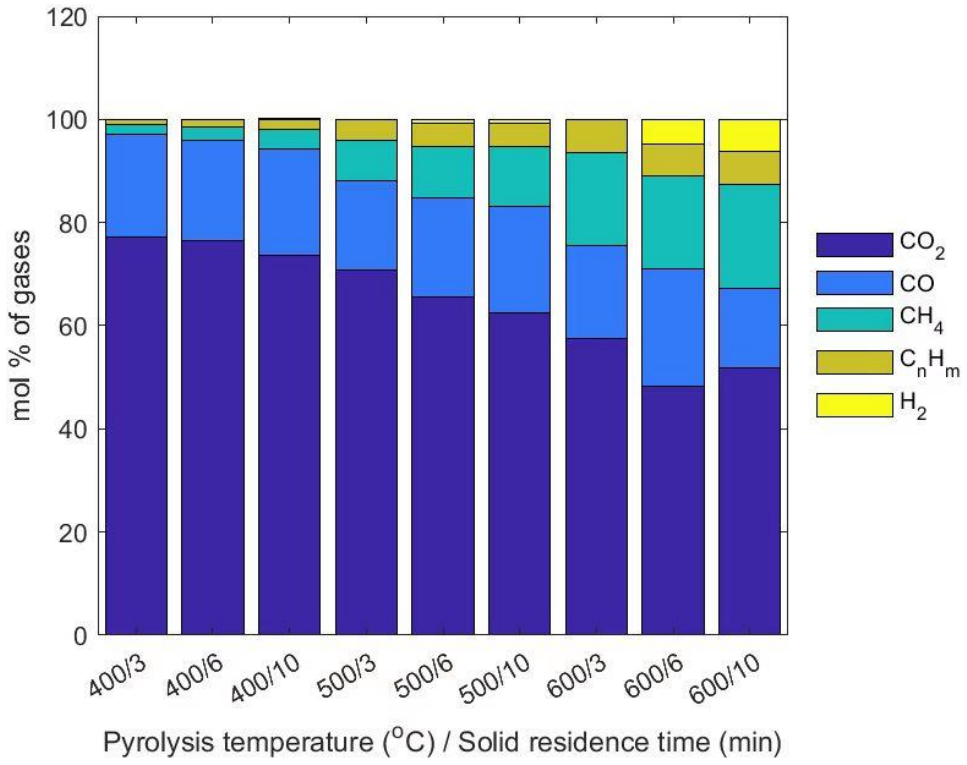

Fig. 5. Distribution of gaseous species (vol.%) from the slow pyrolysis experiments using wheat straw with varying pyrolysis temperature and solid residence time.

The gas product yields had a maximum at the top-right corner of the contour map (Fig. 4). Higher pyrolysis temperature and longer SRT led to higher gas product yield. The yield increased from 17.3 (for 3 min SRT at 400 ºC) to 36.5 wt.% (for 10 min SRT at 600 °C). The distribution of the gaseous species that comprise the gas product from the slow pyrolysis experiments with varying temperature and solid residence time are presented in Fig. 5. CO_2 was the main fraction, comprising at least half of the gas product, followed by CO, CH_4, light hydrocarbons (sum of ethene, ethane, propene and propane) and H_2. Hydrogen gas was only seen in insignificant amounts (≈1 vol.%) when the pyrolysis temperature was below 500 °C), with a considerable increase to ≈5–6 wt.% at 600 °C. The proportion of CO_2 decreased with pyrolysis temperature, while CH_4, other light hydrocarbons and H_2 increased. The fraction of CO did not show a clear trend with temperature. The changes in gas composition with pyrolysis temperature had the positive

consequence of raising the heating value of the gas product since the proportion of combustible gases was increased. Similar trends were found by Yu *et al.* in their study of corn stalks and rice husks in the same auger reactor [17], with CH_4 having a noticeable increase and CO_2 a pronounced decrease. For those feedstocks, a pyrolysis temperature of 500–550 °C was required for significant H_2 production, while CO was seen to increase slowly with pyrolysis temperature.

With increasing SRT, more gas was produced at the expense of the liquid product, which has been reported by other researchers using auger reactors and justified by the occurrence of secondary reactions, including cracking, reforming and dehydration to produce lower molecular weight organics and gases [15]. The reactions involved would cause an increase in the proportion of lower molecular weight gaseous species such as H_2, CH_4, and light hydrocarbons, which was verified by the MicroGC results (Fig. 5). CO_2 was seen to decrease with SRT. The cracking reactions were probably catalysed by the char product (or the inorganic contents), and therefore its yield may not change, which was the case.

According to a TGA study of thermochemical decomposition of lignocellulosic components, Yang et al. found that CO_2 was more connected to primary pyrolysis reactions of cellulose and hemicellulose, while CO and CH_4 originated more from secondary reactions and their proportion increased upon extending the residence time of gaseous products and higher pyrolysis temperature.[26] This explains well the distribution of the gas products in our work.

3.1.4. Statistical analysis of the effects on product yields

Table 2 shows the ANOVA results on the effects of process conditions and feedstock properties on the product yields. The fixed carbon content of feedstock was not included in the analysis as it is a variable dependent on volatile matter and ash contents. The most significant effects of the operating conditions on the product yields are plotted in Fig. 6. The ANOVA analysis

shows that the pyrolysis temperature, SRT and ash content in feedstock were the most important parameters determining the product yields. The effect of pyrolysis temperature was significant ($p < 0.01$) for the yields of all products. Higher pyrolysis temperatures led to lower char yield but higher gas yield. A maximum liquid product yield could be found at 500 ^{o}C. The SRT had a significant effect on the liquid and gas yields but no effect on the char yield, which was confirmed by the experimental results in this study. Longer SRT led to lower liquid yield and higher gas yield. Volatile matter content in feedstock significantly affected ($p < 0.01$) the char yield negatively.

Table 2. Effect of process conditions on the product yields from wheat straw pellets in a continuous auger reactor by ANOVA.

Product yields	Temperature	SRT	Feedstock volatile matter	Feedstock ash
Char	**(-)	ns	**(-)	ns
Liquid	**(-)	**(-)	ns	ns
Gas	**(+)	**(+)	ns	ns

Abbreviations: ns = not significant; ** p value <0.01; (+) positive effect; (-) negative effect.

The modified linear models to predict the yields of char, liquid and gas products are listed as Eq. 1–3. All input variables that had no significant effects ($p > 0.05$) on the responses were excluded from the models. Because the linear regression approach assumes a linear relationship between variables and responses, the ability of the linear models to interpret relationships in complex systems may be limited [27]. However, these models provide a simple method to estimate products yield with limited information. The estimation of char yield was not as accurate as the estimation of liquid and gas yields. The plots of actual and predicted values are shown in Fig. 7. Nevertheless, all three models have good prediction performance.

$$Char\ yield = 96.378 - 0.0275 \times Temp - 0.673 \times VM \qquad R^2=0.7511 \quad (1)$$

$$Liquid\ yield = 63.981 - 0.0302 \times Temp - 0.426 \times SRT \qquad R^2=0.8360 \quad (2)$$

$$Gas\ yield = -15.551 + 0.0716 \times Temp + 0.272 \times SRT \qquad R^2=0.9105 \quad (3)$$

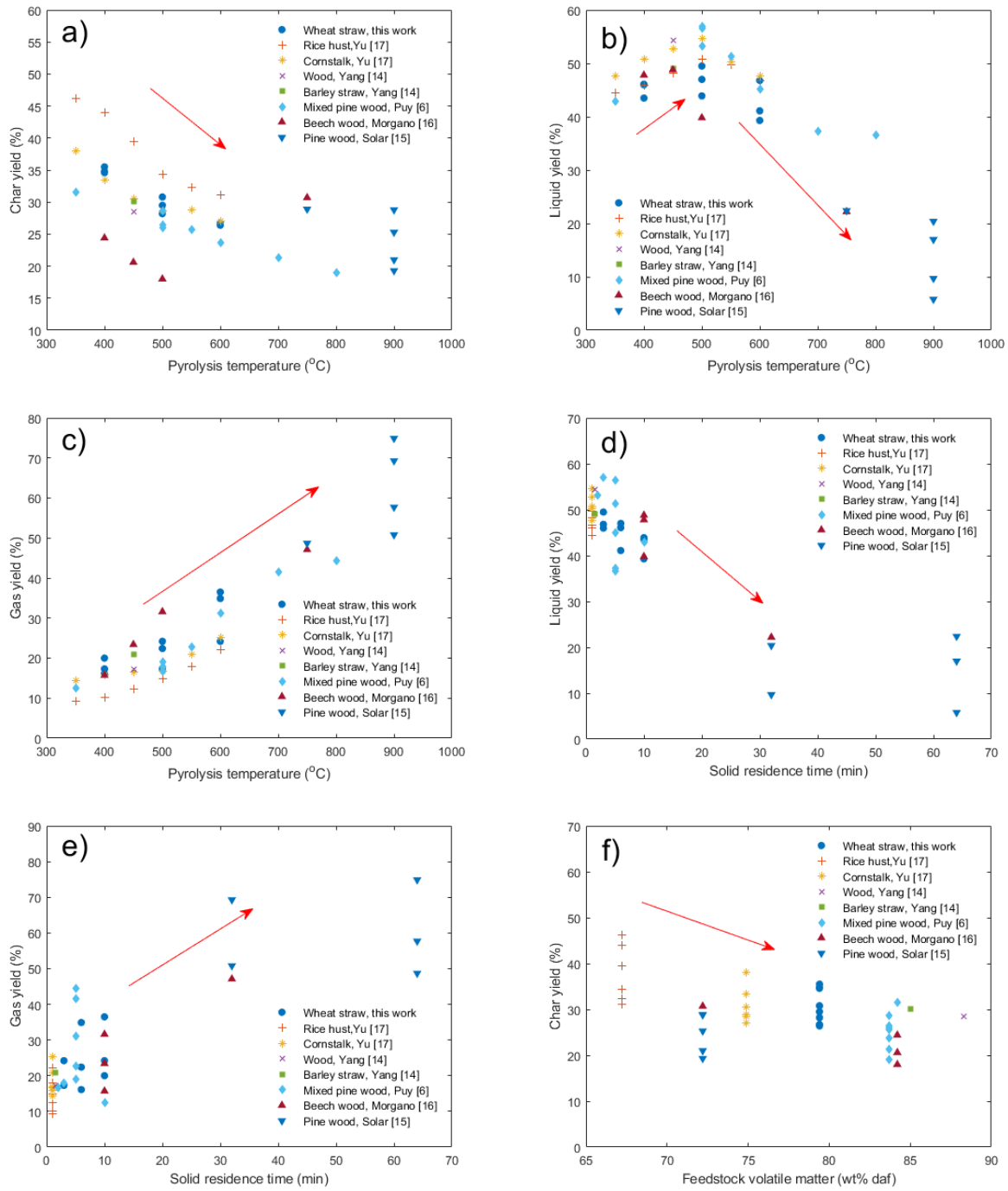

Fig. 6. Effects of the operating conditions on the product yields (a. pyrolysis temperature vs char yield; b. pyrolysis temperature vs liquid yield; c. pyrolysis temperature vs gas yield; d. solid

residence time vs liquid yield; e. solid residence time vs gas yield; f. feedstock volatile matter content vs char yield)

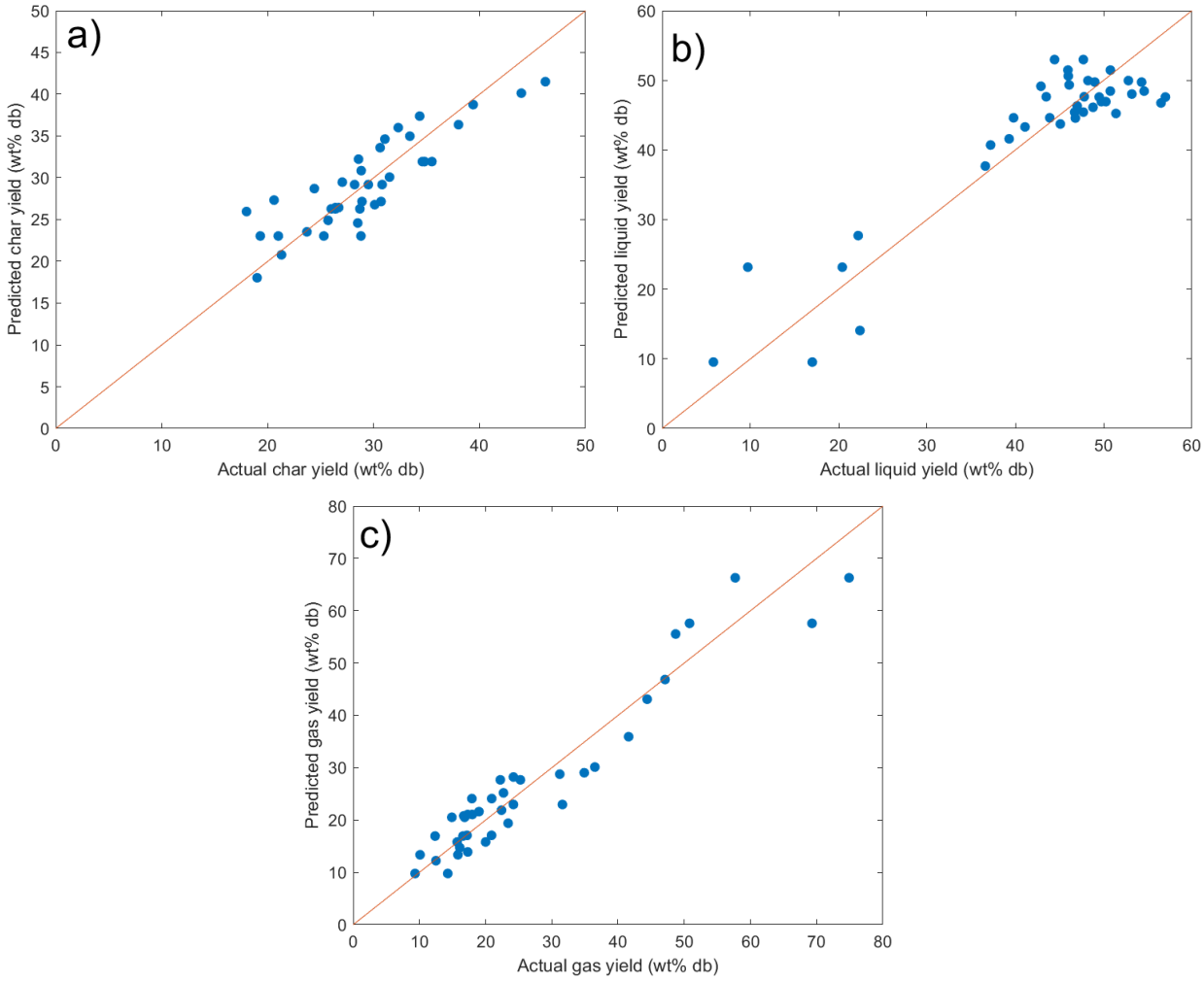

Fig. 7. Comparison between the actual values vs predicted values of the linear models for (a) char yield, (b) liquid yield and (c) gas yield.

3.2. Characterisation of char products

3.2.1. Proximate and ultimate analyses

The proximate and ultimate analyses of the char products are presented in Table 3, along with the calculated higher heating values (HHV). The sulphur content of the char was lower than 0.1 wt.%, so it was not shown.

Table 3. Proximate (wt.%, dry basis) and ultimate analyses (wt.%, dry ash-free basis) and the calculated higher heating value (MJ kg^{-1}, dry basis) of the chars produced from slow pyrolysis of wheat straw pellets.

Pyrolysis temperature (°C)	SRT (min)	Volatile matter	Ash	Fixed carbon [a)]	C	H	N	O [a)]	HHV
400	3	33.4	13.9	52.7	77.6	5.0	1.7	15.6	26.9
	6	32.9	15.0	52.5	76.8	4.5	1.3	17.1	25.7
	10	30.0	12.9	57.1	78.5	4.6	1.3	15.5	26.6
500	3	23.6	13.9	62.5	82.5	4.1	1.5	11.7	27.5
	6	21.5	16.8	61.7	82.9	4.2	1.2	11.6	26.9
	10	20.4	14.4	65.2	83.2	3.8	1.2	11.7	27.1
600	3	17.5	15.0	67.5	87.0	3.4	1.4	8.2	28.1
	6	15.7	17.5	66.8	87.1	3.3	1.3	8.1	27.3
	10	12.9	17.4	69.7	89.7	3.1	1.1	6.0	28.0

a) By difference

An increase in pyrolysis temperature leads to a decrease in the volatile matter in the char product and an increase in the fixed carbon proportion since devolatilisation keeps occurring when the pyrolysis temperature increases. This suggests that the chars produced at higher pyrolysis temperatures could be more appropriate for carbon sequestration in a soil application due to the higher fixed carbon content, which is correlated with the chars' higher recalcitrance and stability [1,28]. The ash proportions also increase with pyrolysis temperature since virtually all the inorganic matter remains in the char as the volatile matter is lost. Since the wheat straw feedstock had a relatively low ash content (4.3 wt.%, dry basis), the resulting chars have lower ash contents when compared with chars from other feedstocks. For example, the corn stalk and rice husk feedstocks pyrolysed by Yu *et al.* had ash contents of around 10 and 16 wt.%, and the resulting chars had ash contents (dry basis) of 20 to 33 wt.%, for corn stalk feedstock, and of 30 to 44 wt.%, for rice husks [17]. Higher ash content is connected to more significant fouling and corrosion risk

when the char is applied for energy production through combustion [29]. Soil applications are also influenced by the ash fraction and its contents [28].

The data from this work and a similar reactor were also analysed. As shown in Fig. 8a, the VM/FC ratio of the char samples, an indicator of coal rank, was a function of pyrolysis temperature, independent of the type of biomass and other operating conditions. The ash content was dependent on the pyrolysis temperature and feedstock ash content (Fig. 8b). Higher temperature and higher ash content in feedstock led to high ash content in produced char.

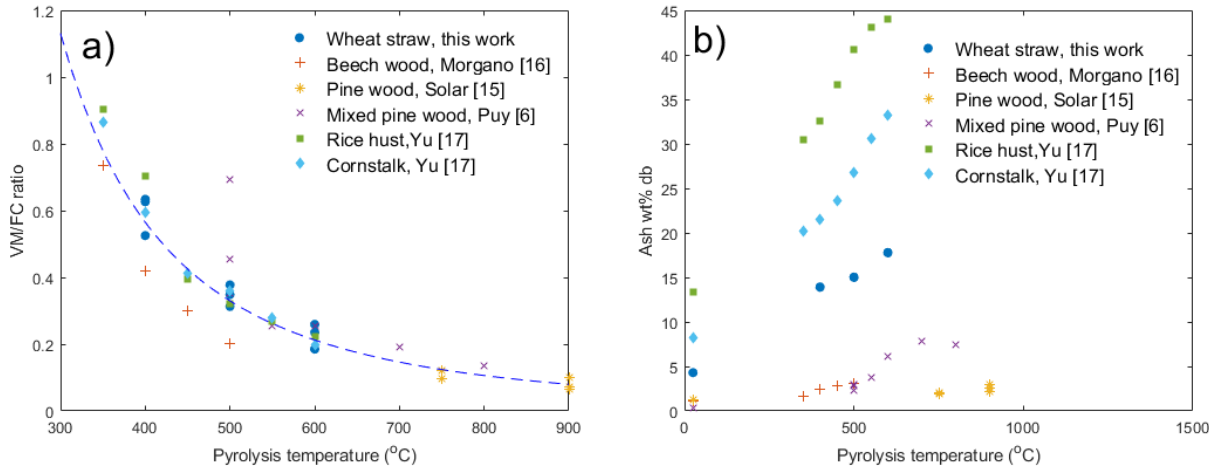

Fig. 8. Effect of pyrolysis temperature on (a) VM/FC ratio and (b) ash content.

Regarding the effect of SRT, it was seen that volatile matter decreased with this parameter for all three pyrolysis temperatures tested. This effect was also reported by Puy *et al.* for SRT between 1.5 and 5 minutes [6]. This was related to a higher exposure time of the char product to the pyrolysis vapours, which can continue secondary reactions with the char surface. The effect of SRT on ash proportion seemed positive, but this trend was more challenging to ascertain.

The carbon proportion in the chars increased with pyrolysis temperature, while hydrogen decreased. As a result of this and oxygen fraction decreasing, the char heating value increased since the ash content increased. However, it was not as significant as the effects on the elemental proportions. The increase in carbon proportion and decrease in hydrogen and oxygen relates to the

reactions happening during the pyrolysis process, e.g. dehydration (removal of hydroxyl groups) and decarboxylation (removal of carboxyl and carbonyl groups) [30]. The trends of elemental composition with pyrolysis temperature indicate that the char's resistance to degradation (related to the O/C ratio) and aromaticity (related to the H/C ratio) was increased [31]. The solid residence time did not have such a noticeable effect on the elemental distribution of the char products. However, with some exceptions, the carbon proportion increased whilst the hydrogen and oxygen fractions decreased, which can be correlated to the decrease in the volatile matter and was attributed to more secondary reactions taking place for greater SRT. This was verified by Solar *et al.*, using pine wood (0.5–2.0 mm size) in an auger reactor (750–900 °C): the carbon content of the char product increased when the SRT was raised from 32 to 64 minutes [15].

To evaluate the carbonisation process, H/C and O/C atomic ratios of the feedstock and their derived char were plotted in a van Krevelen diagram (Fig. 9b). The slow pyrolysis of lignocellulosic biomass is mainly a dehydration process accompanied by decarboxylation. It is interesting to see that the H/C ratio of the chars was a function of temperature despite different feedstocks and reactors (Fig. 9c), whilst the O/C ratio of the char was relevant to the pyrolysis temperature and O/C ratio of the feedstock (Fig. 9a).

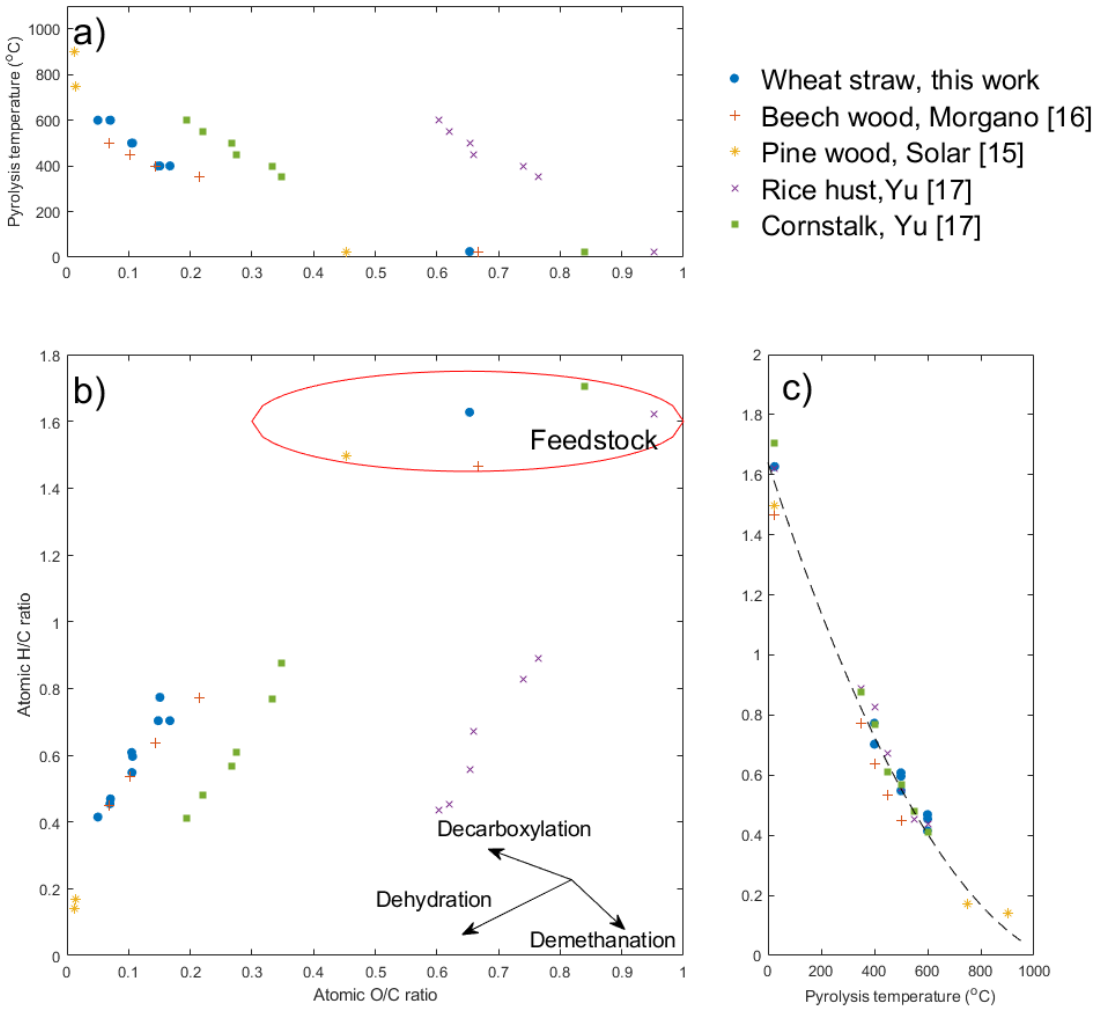

Fig. 9. (a) van Krevelen diagram (b) H/C ratio vs pyrolysis temperature (c) O/C ratio vs pyrolysis temperature.

Compared with the wheat straw feedstock (19.2 MJ kg^{-1}, in Table 1), the heating value was significantly increased, to an average for all chars of 26.5 MJ kg^{-1} (± 1.5 MJ kg^{-1}). The slow pyrolysis process has thus created a char product significantly more valuable for energy generation (e.g., through combustion), mainly by decreasing the oxygen content. The results are comparable with those obtained from fixed bed slow pyrolysis of straw pellets by Ronsse *et al.* [32]. In that study, for chars produced at 450 and 600 °C, the HHVs were between 25 and 26 MJ kg^{-1}. In a

study performed with the same auger reactor as in this work [17], corn stalk and rice husk chars (350–600 °C) had lower HHV than the wheat straw chars in this present work, especially the rice husk chars. The HHV for the corn stalk chars was 19.9–26.0 MJ kg^{-1}, while the rice husk chars were 17.1–21.3 MJ kg^{-1}. This can be explained mainly by the higher ash content in these feedstocks (around 10 and 16 wt.%, dry basis, respectively) [17]. This shows the greater value that the wheat straw feedstock possesses for energy production through combustion compared with other herbaceous feedstocks. The obtained char HHV is comparable to or even higher than the HHV of some types of coals [33]. The chars produced at higher pyrolysis temperatures have a greater heating value than those from lower temperatures, although the effect is insignificant. The solid residence time did not produce a clear trend on the HHV of the chars.

3.2.2. N_2 porosimetry

The chars were evaluated in terms of their surface area with nitrogen porosimetry at 77 K and BET theory, which yielded surface areas under 15 m^2 g^{-1}. There was no relevant effect of the studied process conditions on the char surface areas. The maximum temperature of 600 °C was not enough to develop porosity, which other researchers have seen. Values reported in the literature for char surface areas vary depending on the conditions used and range from lower than 10 to values over 2000 m^2 g^{-1} [34]. Similar low values of surface area (8.1 m^2 g^{-1}) have been reported for chars from different feedstocks (poultry litter, vine prunings, orange pomace, and seaweed) and produced at temperatures up to 600 °C in a fixed bed reactor [35]. In a study with agricultural residues by Fu *et al.* [36], char surface areas only reached values above 20 m^2 g^{-1} when pyrolysis temperatures were above 800 or 900 °C, depending on the feedstock. Low surface areas indicate that most pores are blocked or very narrow, restricting nitrogen adsorption at 77 K [37]. The ash content of the feedstock was found by Ronsse *et al.* [32] to be correlated with low surface areas in

chars produced from wood biomass and other biomass with high ash contents, such as wheat straw and algae. In that study, at a pyrolysis temperature of 600 °C, the woody feedstock (low ash content of 0.2 wt.%) produced chars with a surface area of up to 127 m^2 g^{-1}, while the chars from wheat straw (7.9 wt.% ash content) and the algae (38.4 wt.% ash content) had a surface area of 22 and 19 m^2 g^{-1}, respectively. The inorganic contents could be deposited in the pores after being molten and re-fused. In the present study, however, the ash content of the wheat straw feedstock is not significantly high (4.3 wt.%, in Table 1), so this effect would not be as noticeable. However, the effect of pore-blocking could be increased during pyrolysis due to the lack of carrier gas, which increases vapour residence time and the contact time between the chars and the produced vapours. The higher contact time could potentially promote the entrapment of volatiles within the char matrix and consequent closure of the char pores.

3.2.3. pH of char products (in H_2O)

The results of the pH analysis of the chars from the experiments with varying temperature and solid residence time can be seen in Fig. 10. Error bars represent standard deviation.

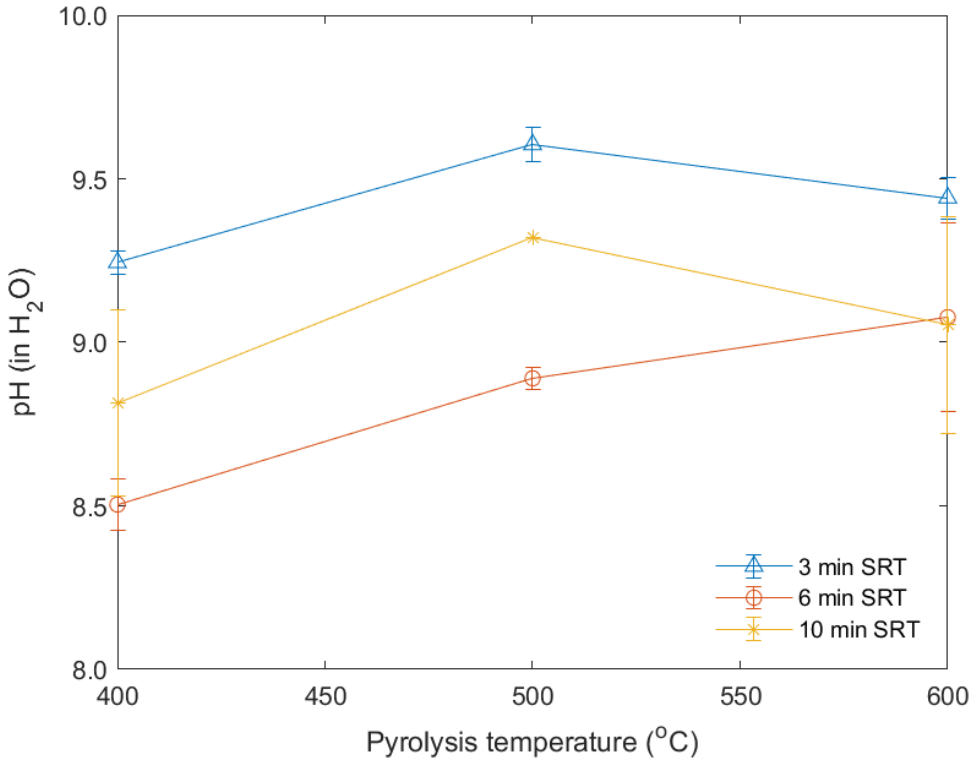

Fig. 10. pH (in H_2O) of the produced chars with varying temperature and solid residence time.

The pH values were situated in the range 8.5–9.6, indicating a basic character of the chars and an increase of pH compared to the wheat straw feedstock, which had a pH (in H_2O) of 7.3. The pH of the chars produced from the as-received wheat straw pellets shows an increase with pyrolysis temperature. An increase of char pH with pyrolysis temperature was also seen for several feedstocks, for example, by Ronsse *et al.* [32], which also verified that chars from pine wood had lower pH than wheat straw, green waste and algae chars. The pH values obtained in that study for wheat straw chars were in the range of 9.8–11.3 (450–600 °C pyrolysis temperature). Similar pH values, between 9.0 and 10.0, were obtained by Budai *et al.* for chars from corn cob and Miscanthus produced in a retort at 400 to 600 °C [38]. The original feedstocks had a pH between 5.0 and 6.0, and the increase was correlated to the loss of volatiles during pyrolysis, which reduced surface functionalities. In the work of Tag *et al.* [35], feedstocks with a higher ash content were found to produce chars with greater pH values. In terms of the influence of solid residence time

for conditions used in the present work, the observed trend on char pH was 3 min > 10 min > 6 min. This does not correlate with the variation of char ash content with SRT (highest for 6 min SRT; in Table 3) unless the ash has an acidic character. Chars with basic character can be used in soil applications to reduce acidity in poor-quality soils, e.g. to rehabilitate former mine grounds [39]. Furthermore, chars with relatively high (basic) pH values have been found to reduce the mobility of heavy metals in soils [40].

3.2.4. FTIR analysis

The char products from slow pyrolysis of wheat straw pellets were further analysed using FTIR to assess the presence of chemical functionalities on the surface. Fig. 11 presents the spectra for the chars from the experiments using the wheat straw feedstock, as well as the feedstock's spectrum for comparison. The spectra correspond to chars produced with 10 minutes SRT. Since IR manifestation of the char materials was not significant for the region of wavenumbers 4000–2000 cm^{-1}, the spectra shown here only have the region of 2000–400 cm^{-1} wavenumbers. The peaks/bands present in the spectra were assigned to the surface chemical functionalities [37,41–43].

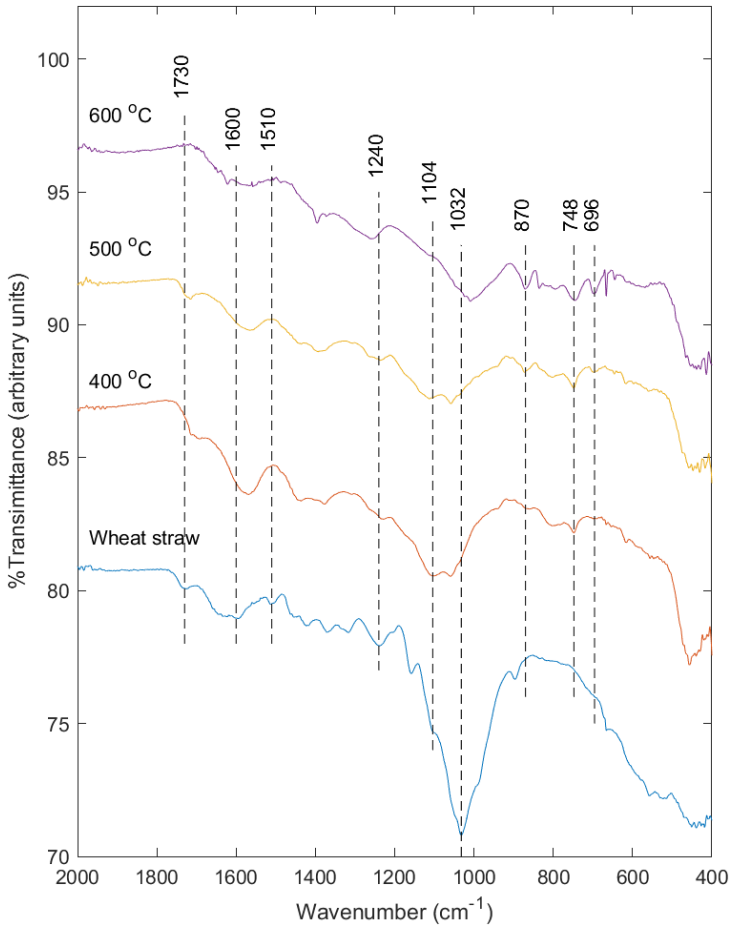

Fig. 11. FTIR spectra for the wheat straw feedstock and chars produced from slow pyrolysis with 10 minutes SRT.

The FTIR spectra showed a reduction of chemical functionalities between the chars and the feedstock, especially in the regions corresponding to O–H (band centred around 3300 cm^{-1}), aliphatic C–H_n (3000–2850 and 1200–1500 cm^{-1}), and C–O (1150–1050 cm^{-1}) bond vibrations. Overall, for the slow pyrolysis chars, the spectra had only relevant IR manifestation for wavenumbers in the region 1800–400 cm^{-1}. The reduction in chemical functionalities is connected to a loss of surface chemical compounds in the form of volatiles and the development of an aromatic structure on the char product's surface when exposed to higher temperatures under pyrolysis conditions [41,44]. The C–O bonds present in the feedstock and significantly reduced in the chars can be attributed to carboxylic and ester groups and aromatic rings, while the aliphatic

$C–H_n$ bonds originate from the feedstock lignocellulosic biopolymers and fatty acids [45,46]. In the work of Tag *et al.*, the FTIR spectra for the chars produced from agricultural residues at the highest studied temperature of 600 °C were considered to be similar to that of graphite (practically no IR manifestation) [35]. Fu *et al.* considered this graphitisation to occur only at pyrolysis temperatures above 800 °C for chars from agricultural residues [36]. The increasing upwards drift in the region 1200–400 cm^{-1} for the char produced at 600 °C was a baseline drift, which has been identified by other authors and attributed to an increase in carbonisation degree from high temperature [37].

The impact of solid residence time is not shown here since there were no significant feature changes with different SRTs. Therefore, the temperature was the only parameter that significantly affected the IR manifestation of the slow pyrolysis chars produced from the as-received wheat straw feedstock. The lack of effect of SRT on the surface functional groups can be correlated to the fact that this parameter was seen to not significantly change the elemental composition of the produced chars (Table 3).

A noticeable change with pyrolysis temperature is the absence of IR manifestation in the wavenumber region 1750–1650 cm^{-1}, corresponding to carbonyl (C=O) stretching bond vibrations, in the spectra of the chars produced at 600 °C. This peak was present for both feedstock and chars produced at 400 and 500 °C, and from both as-received feedstock and feedstock after disintegration by soaking with water. This effect was seen by Chen *et al.* for chars produced from pine needles when the employed pyrolysis temperature was higher than 500 °C [43]. For the chars produced at 600 °C, more functionalities were present in the region 900–600 cm^{-1} ($C–H_n$ bending bond vibrations, out-of-plane), which were indicative of an increase in aromatic features on the char surface as a consequence of the higher pyrolysis temperature [41].

The changes in chemical surface features (e.g. polar groups) impact the basic/acidic character of the char's surface and its hydrophobicity and therefore influences potential applications [47]. The interaction of the char with a cationic compound can be improved if the basicity of the char is increased, e.g. by introducing –OH functionalities on the surface [5]. Functional surface groups containing oxygen, such as –OH and –COOH, can act as binding sites for heavy metals, for example, through complexation [48], which benefits liquid-phase adsorption and soil applications. The processing of the wheat straw at lower pyrolysis temperatures can therefore possess advantages for these applications in relation to higher pyrolysis temperatures since some potentially advantageous chemical functionalities remain.

3.2.5 Microscopic analyses with SEM

The produced chars at different temperatures with a SRT of 3 minutes were analysed with Scanning Electron Microscopy (SEM) to assess morphological features at microscopic level. Examples of micrographs of the chars from slow pyrolysis of wheat straw with varying pyrolysis temperature are presented in Fig. 12. The pictures on the left correspond to zoomed-in areas from the pictures on the left. The highlighted pore in the zoomed-in area of the 600 °C char micrograph has a diameter of ≈3.6 µm, according to SEM measurement.

The size of microscopic particles varied significantly, generally ranging 0.5-300 µm, with fractures seen on some particles, especially the larger ones. Particles were irregularly shaped, some with rough external surfaces and others with smoother surfaces. The particle sizes and shapes were influenced by the post-production grinding and sieving of the char (425 µm sieve). The char particles produced at the lowest temperature possessed smoother surfaces and less fractures compared to chars from 500 and 600 °C. This could be related to lignin, which goes through

different processes such as softening, plasticisation and glass transition, depending on temperature[37].

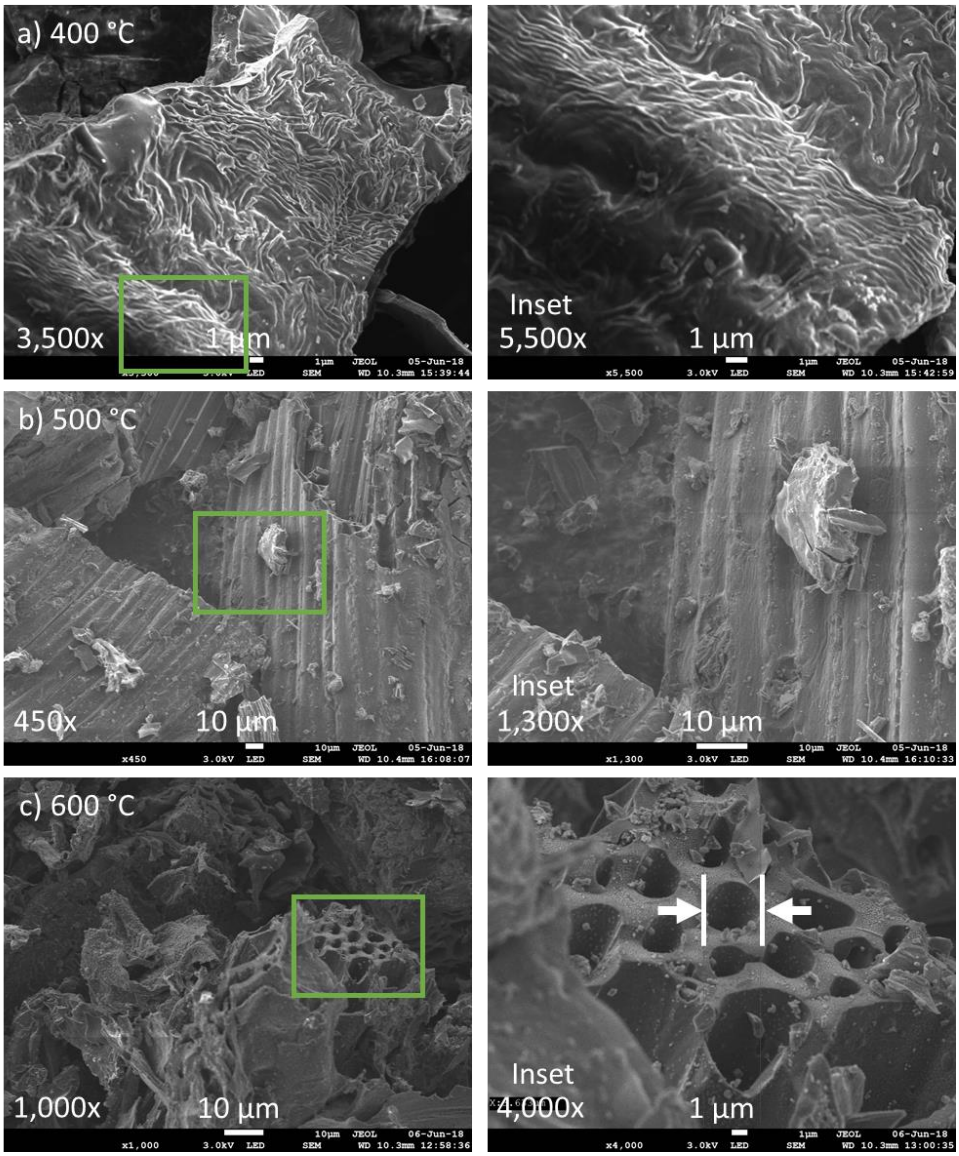

Fig. 12. SEM micrographs of chars produced at (a) 400, (b) 500 and (c) 600 °C in the screw reactor with 3 minutes SRT and no carrier gas. Zoomed-in areas highlighted in green rectangles are depicted on the right. The highlighted pore has ≈3.6 µm diameter.

Pores were seen on some particles, which appeared to be channels from the original lignocellulosic matrix of the feedstock, through which the plant would conduct water and nutrients through. The micrographs suggest the pyrolysis process did not produce new pores besides the already existing ones from the biomass skeletal structure, and process temperature had little effect on microscopic appearance. This was in line with the results obtained from N_2 porosimetry, which showed low porosity development regardless of process temperature.

3.2.6. Statistical analysis of the effects on product's properties

Table 4. Effect of process conditions on the product yields from wheat straw pellets in a continuous auger reactor by ANOVA.

	Pyrolysis temperature	SRT	Feedstock volatile matter	Feedstock ash
VM	**(-)	ns	*(-)	**(-)
FC	**(+)	ns	ns	*(-)
Ash	**(+)	*(-)	ns	**(+)
HHV	**(+)	ns	**(+)	ns

Abbreviations: ns = not significant; * 0.01 < p value < 0.05; ** p value < 0.01; (+) positive effect; (-) negative effect.

Table 4 shows the ANOVA results on the effects of process conditions and feedstock properties on the product's properties. Pyrolysis temperature was the most critical parameter. It had significant ($p<0.01$) effects on all study responses, including the char's volatile matter, fixed carbon, ash content and HHV values. Increasing the pyrolysis temperature would reduce the volatile matter in the produced char but increase the char's fixed carbon, ash content and HHV. Ash content in the feedstock is the second most important parameter. It had a significant negative effect ($p<0.01$) on the volatile matter in char, a significant positive effect ($p<0.01$) on the ash content in char, and a less significant negative effect ($0.01<p<0.05$) on the fixed carbon. However,

the ash content in feedstock had no significant effect on the char's HHV. The volatile matter in the feedstock had a significant positive effect on char HHV and a less significant adverse effect on the volatile matter in the produced char. SRT was a less critical parameter, which only had a negative effect on the produced char's ash content. The most important operating conditions that affected the product yields are plotted in Fig. 13.

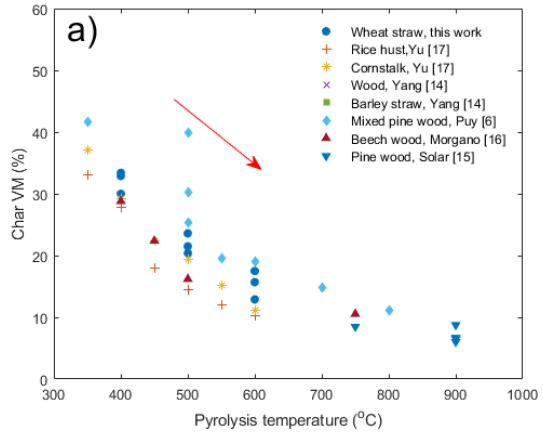
a)
Char VM (%)
Pyrolysis temperature (°C)
Wheat straw, this work
Rice hust,Yu [17]
Cornstalk, Yu [17]
Wood, Yang [14]
Barley straw, Yang [14]
Mixed pine wood, Puy [6]
Beech wood, Morgano [16]
Pine wood, Solar [15]

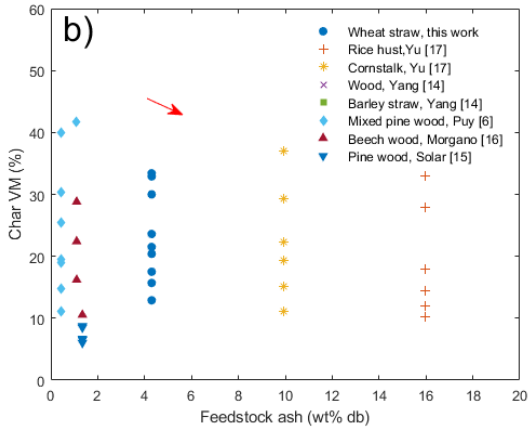
b)
Char VM (%)
Feedstock ash (wt% db)
Wheat straw, this work
Rice hust,Yu [17]
Cornstalk, Yu [17]
Wood, Yang [14]
Barley straw, Yang [14]
Mixed pine wood, Puy [6]
Beech wood, Morgano [16]
Pine wood, Solar [15]

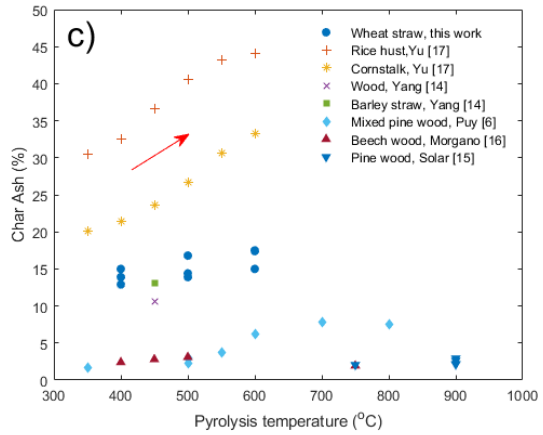
c)
Char Ash (%)
Pyrolysis temperature (°C)
Wheat straw, this work
Rice hust,Yu [17]
Cornstalk, Yu [17]
Wood, Yang [14]
Barley straw, Yang [14]
Mixed pine wood, Puy [6]
Beech wood, Morgano [16]
Pine wood, Solar [15]

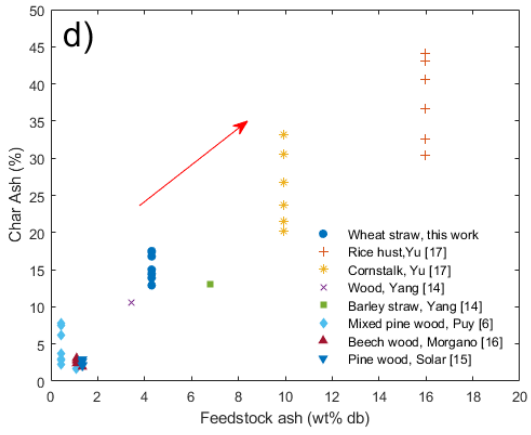
d)
Char Ash (%)
Feedstock ash (wt% db)
Wheat straw, this work
Rice hust,Yu [17]
Cornstalk, Yu [17]
Wood, Yang [14]
Barley straw, Yang [14]
Mixed pine wood, Puy [6]
Beech wood, Morgano [16]
Pine wood, Solar [15]

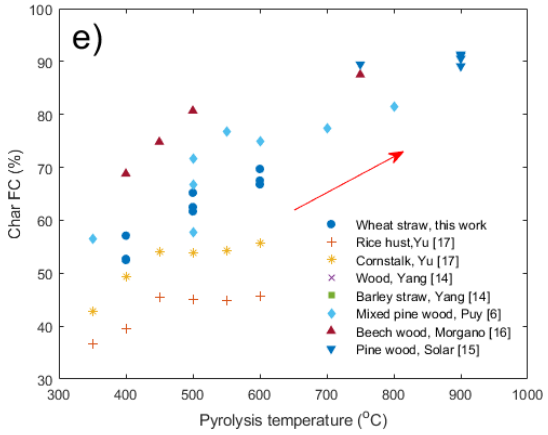
e)
Char FC (%)
Pyrolysis temperature (°C)
Wheat straw, this work
Rice hust,Yu [17]
Cornstalk, Yu [17]
Wood, Yang [14]
Barley straw, Yang [14]
Mixed pine wood, Puy [6]
Beech wood, Morgano [16]
Pine wood, Solar [15]

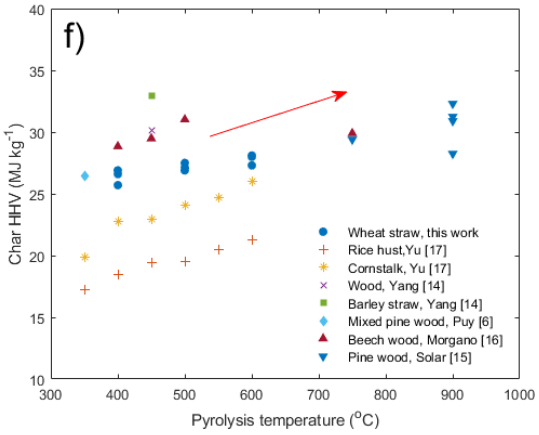
f)
Char HHV (MJ kg-1)
Pyrolysis temperature (°C)
Wheat straw, this work
Rice hust,Yu [17]
Cornstalk, Yu [17]
Wood, Yang [14]
Barley straw, Yang [14]
Mixed pine wood, Puy [6]
Beech wood, Morgano [16]
Pine wood, Solar [15]

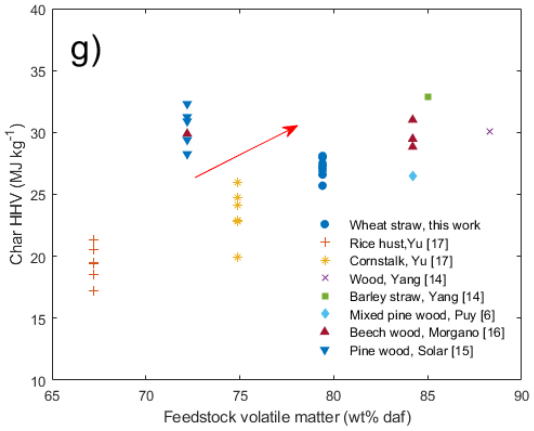

Fig. 13. Effects of the operating conditions on the product yields (a. pyrolysis temperature vs char's VM; b. feedstock ash vs char's VM; c. pyrolysis temperature vs char's ash; d. feedstock ash vs char's ash; e. pyrolysis temperature vs char's FC; f. Pyrolysis temperature vs char's HHV; g. feedstock volatile matter vs char HHV)

The modified linear modules to predict the char properties, including volatile matter, fixed carbon, ash content and HHV, are listed as Eq. 4–7. Like the models for the product yields, all input variables that had no significant effects were removed. The plots of actual and predicted values are shown in Fig. 14. Again, all four models have good prediction performance.

$$Char\ VM = 117.150 - 0.0710 \times Temp - 0.652 \times feedstock\ VM - 1.286 \times feedstock\ Ash$$

R^2=0.8090 (4)

$$Char\ FC = 43.131 + 0.0553 \times Temp - 1.710 \times feedstock\ Ash$$

R^2=0.9250 (5)

$$Char\ Ash = -4.343 + 0.0167 \times Temp - 0.189 \times SRT + 2.219 \times feedstock\ Ash$$

R^2=0.9447 (6)

$$Char\ HHV = -30.917 + 0.0196 \times Temp + 0.610 \times feedstock\ VM$$

R^2=0.9193 (7)

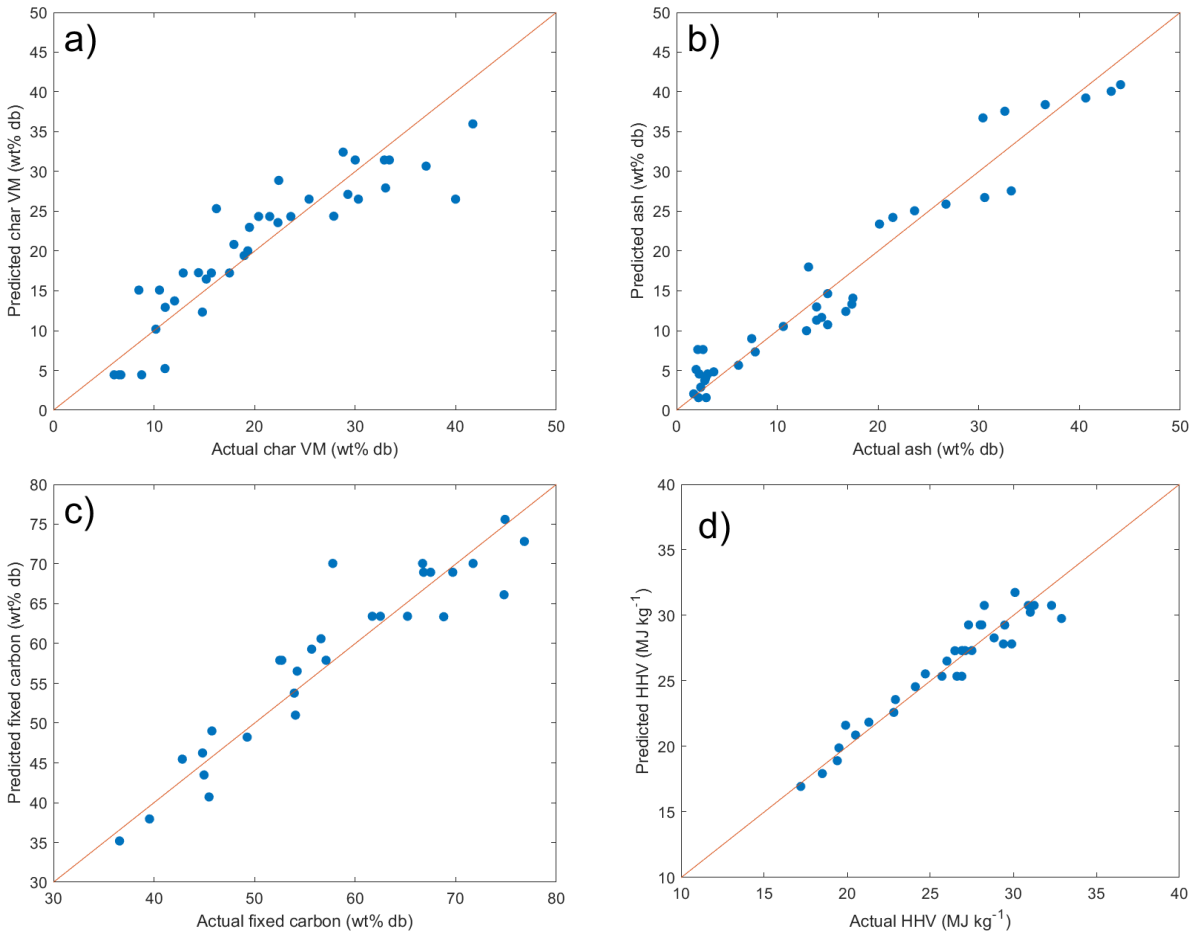

Fig. 14. Comparison between the actual values vs predicted values of the linear models for (a) char's VM, (b) ash, (c) fixed carbon and (d) HHV.

4. Conclusions

Chars were produced from wheat straw in a continuous auger reactor with varying temperature and solid residence time, which had different effects on the product yields and char properties. Pyrolysis temperature was the dominant variable in determining product distribution, with a more significant effect than solid residence time. As expected, char yields decreased with temperature, while gas yields increased. The statistical analysis confirmed the findings. Linear models were developed to predict the yields of the products from slow pyrolysis with reasonable accuracy, R^2 values greater than 0.75.

The properties of the chars were also affected by the process parameters, especially by pyrolysis temperature. An increase in carbon content and decrease in oxygen content with increasing pyrolysis temperature increased the char's calorific value. Higher solid residence time caused a reduction in the volatile matter of the char, which could be due to secondary reactions. The linear models developed were able to predict the char properties, including volatile matter, fixed carbon, ash content and HHV. Apart from the volatile matter, the prediction of the other three char properties had R^2 values greater than 0.91.

The results from the experimental investigation and the linear models can be used to design and optimise char production by slow pyrolysis.

Declaration of Competing Interest

The authors declare that they have no known competing financial interests or personal relationships that could have influenced the work reported in this paper.

Acknowledgements

This project has received funding from the European Union's Horizon 2020 research and innovation programme under the Marie Skłodowska-Curie grant agreement No. 721991 (GreenCarbon). The work was also supported by an Institutional Links grant (No. 527641843), under the Turkey partnership. The grant is funded by the UK Department for Business, Energy and Industrial Strategy and delivered by the British Council.

CRediT author statement

Filipe Rego: Investigation, Writing - Original Draft, Formal analysis; Huan Xiang: Formal analysis, Writing - Review & Editing; Yang Yang: Conceptualisation, Funding acquisition, Writing - Review & Editing; Jiawei Wang: Writing - Review & Editing, Supervision, Funding acquisition; Jorge López Ordovás: Writing - Review & Editing; Katie Chong: Writing - Review & Editing, Anthony Bridgwater: Supervision, Writing - Review & Editing, Funding acquisition

References

[1] J.J. Manyà, Pyrolysis for biochar purposes: A review to establish current knowledge gaps and research needs, Environ. Sci. Technol. 46 (2012) 7939–7954. https://doi.org/10.1021/es301029g.

[2] C. Di Stasi, D. Alvira, G. Greco, B. González, J.J. Manyà, Physically activated wheat straw-derived biochar for biomass pyrolysis vapors upgrading with high resistance against coke deactivation, Fuel. 255 (2019) 115807. https://doi.org/10.1016/j.fuel.2019.115807.

[3] F. Guo, X. Li, Y. Liu, K. Peng, C. Guo, Z. Rao, Catalytic cracking of biomass pyrolysis tar over char-supported catalysts, Energy Convers. Manag. 167 (2018) 81–90. https://doi.org/10.1016/j.enconman.2018.04.094.

[4] M.G. Plaza, C. Pevida, C.F. Martín, J. Fermoso, J.J. Pis, F. Rubiera, Developing almond shell-derived activated carbons as CO2 adsorbents, Sep. Purif. Technol. 71 (2010) 102–106. https://doi.org/10.1016/J.SEPPUR.2009.11.008.

[5] Y. Zhu, B. Yi, Q. Yuan, Y. Wu, M. Wang, S. Yan, Removal of methylene blue from aqueous solution by cattle manure-derived low temperature biochar, RSC Adv. 8 (2018) 19917–19929. https://doi.org/10.1039/c8ra03018a.

[6] N. Puy, R. Murillo, M. V Navarro, J.M. López, J. Rieradevall, G. Fowler, I. Aranguren, T. García, J. Bartrolí, A.M. Mastral, Valorisation of forestry waste by pyrolysis in an auger

reactor, Waste Manag. 31 (2011) 1339–1349. https://doi.org/10.1016/j.wasman.2011.01.020.

[7] P.C. Badger, P. Fransham, Use of mobile fast pyrolysis plants to densify biomass and reduce biomass handling costs - A preliminary assessment, Biomass and Bioenergy. 30 (2006) 321–325. https://doi.org/10.1016/j.biombioe.2005.07.011.

[8] A.V. Bridgwater, Review of fast pyrolysis of biomass and product upgrading, Biomass and Bioenergy. 38 (2012) 68–94. https://doi.org/10.1016/j.biombioe.2011.01.048.

[9] M.K. Bahng, C. Mukarakate, D.J. Robichaud, M.R. Nimlos, Current technologies for analysis of biomass thermochemical processing: A review, Anal. Chim. Acta. 651 (2009) 117–138. https://doi.org/10.1016/j.aca.2009.08.016.

[10] J.D. Martínez, R. Murillo, T. García, A. Veses, Demonstration of the waste tire pyrolysis process on pilot scale in a continuous auger reactor, J. Hazard. Mater. 261 (2013) 637–645. https://doi.org/10.1016/j.jhazmat.2013.07.077.

[11] A. Hornung, W. Koch, H. Seifert, Haloclean and PYDRA - a dual staged pyrolysis plant for the recycling waste electronic and electrical equipment (WEEE), in: Met. Energy Recover. Internat.Symp.in North. Sweden, Skelleftea, 2003: p. 7.

[12] Y. Yang, S. Heaven, N. Venetsaneas, C.J. Banks, A. V. Bridgwater, V.A. Bridgwater, Slow pyrolysis of organic fraction of municipal solid waste (OFMSW): Characterisation of products and screening of the aqueous liquid product for anaerobic digestion, Appl. Energy. 213 (2018) 158–168. https://doi.org/10.1016/j.apenergy.2018.01.018.

[13] M. Ouadi, N. Jaeger, C. Greenhalf, J. Santos, R. Conti, A. Hornung, Thermo-Catalytic Reforming of municipal solid waste, Waste Manag. 68 (2017) 198–206. https://doi.org/10.1016/j.wasman.2017.06.044.

[14] Y. Yang, J.G. Brammer, A.S.N.N. Mahmood, A. Hornung, Intermediate pyrolysis of biomass energy pellets for producing sustainable liquid, gaseous and solid fuels, Bioresour. Technol. 169 (2014) 794–799. https://doi.org/10.1016/j.biortech.2014.07.044.

[15] J. Solar, I. de Marco, B.M. Caballero, A. Lopez-Urionabarrenechea, N. Rodriguez, I. Agirre, A. Adrados, Influence of temperature and residence time in the pyrolysis of woody biomass waste in a continuous screw reactor, Biomass and Bioenergy. 95 (2016) 416–423. https://doi.org/10.1016/j.biombioe.2016.07.004.

[16] M. Tomasi Morgano, H. Leibold, F. Richter, H. Seifert, Screw pyrolysis with integrated sequential hot gas filtration, J. Anal. Appl. Pyrolysis. 113 (2015) 216–224. https://doi.org/10.1016/j.jaap.2014.12.019.

[17] Y. Yu, Y. Yang, Z. Cheng, P.H. Blanco, R. Liu, A. V Bridgwater, J. Cai, V.A. Bridgwater, J. Cai, Pyrolysis of Rice Husk and Corn Stalk in Auger Reactor. 1. Characterization of Char and Gas at Various Temperatures, Energy and Fuels. 30 (2016) 10568–10574. https://doi.org/10.1021/acs.energyfuels.6b02276.

[18] C.M. Roggero, V. Tumiatti, A. Scova, C. De Leo, A. Binello, G. Cravotto, Characterization of oils from haloclean pyrolysis of biomasses, Energy Sources, Part A Recover. Util. Environ. Eff. 33 (2011) 467–476. https://doi.org/10.1080/15567030903096980.

[19] D.L. Dalluge, T. Daugaard, P. Johnston, N. Kuzhiyil, M.M. Wright, R.C. Brown, Continuous production of sugars from pyrolysis of acid-infused lignocellulosic biomass, Green Chem. 16 (2014) 4144–4155. https://doi.org/10.1039/c4gc00602j.

[20] W.F. Fassinou, L. de Steene, S. Toure, G. Volle, P. Girard, Pyrolysis of Pinus pinaster in a two-stage gasifier: Influence of processing parameters and thermal cracking of tar, Fuel Process. Technol. 90 (2009) 75–90. https://doi.org/10.1016/j.fuproc.2008.07.016.

[21] M. Tripathi, J.N. Sahu, P. Ganesan, Effect of process parameters on production of biochar from biomass waste through pyrolysis: A review, Renew. Sustain. Energy Rev. 55 (2016) 467–481. https://doi.org/10.1016/j.rser.2015.10.122.

[22] ASTM, ASTM International, E1131-08 Standard Test Method for Compositional Analysis by Thermogravimetry, Annu. B. ASTM Stand. (2008) 8–12. https://doi.org/10.1520/E1131-08.

[23] S.A. Channiwala, P.P. Parikh, A unified correlation for estimating HHV of solid, liquid and gaseous fuels, Fuel. 81 (2002) 1051–1063. https://doi.org/10.1016/S0016-2361(01)00131-4.

[24] ASTM D 1762-84, Standard Test Method for Chemical Analysis of Wood Charcoal., ASTM Int. 84 (2011) 1–2. https://doi.org/10.1520/D1762-84R07.

[25] U. Hornung, D. Schneider, A. Hornung, V. Tumiatti, H. Seifert, Sequential pyrolysis and catalytic low temperature reforming of wheat straw, J. Anal. Appl. Pyrolysis. 85 (2009) 145–150. https://doi.org/10.1016/j.jaap.2008.11.006.

[26] H. Yang, R. Yan, H. Chen, D.H. Lee, C. Zheng, Characteristics of hemicellulose, cellulose and lignin pyrolysis, Fuel. 86 (2007) 1781–1788. https://doi.org/10.1016/J.FUEL.2006.12.013.

[27] K.S. Ro, J.R.V. Flora, S. Bae, J.A. Libra, N.D. Berge, A. Álvarez-Murillo, L. Li, Properties of Animal-Manure-Based Hydrochars and Predictions Using Published Models, ACS Sustain. Chem. Eng. 5 (2017) 7317–7324. https://doi.org/10.1021/acssuschemeng.7b01569.

[28] S. Sohi, E. Lopez-Capel, E. Krull, R. Bol, Biochar's roles in soil and climate change: A review of research needs, 2009.

[29] M. Holubcik, J. Jandacka, M. Malcho, Ash Melting Temperature Prediction from Chemical Composition of Biomass Ash, Holist. Approach to Environ. 5 (2015) 119–125.

[30] K. Jindo, H. Mizumoto, Y. Sawada, T. Sonoki, Physical and chemical characterization of biochars derived from different agricultural residues, Biogeosciences. (2014) 6613–6621. https://doi.org/10.5194/bg-11-6613-2014.

[31] K. Crombie, O. Mašek, S.P. Sohi, P. Brownsort, A. Cross, The effect of pyrolysis conditions on biochar stability as determined by three methods, GCB Bioenergy. 5 (2013) 122–131. https://doi.org/10.1111/gcbb.12030.

[32] F. Ronsse, S. van Hecke, D. Dickinson, W. Prins, Production and characterization of slow pyrolysis biochar: Influence of feedstock type and pyrolysis conditions, GCB Bioenergy. 5 (2013) 104–115. https://doi.org/10.1111/gcbb.12018.

[33] P. Tan, C. Zhang, J. Xia, Q. Fang, G. Chen, Estimation of higher heating value of coal based on proximate analysis using support vector regression, Fuel Process. Technol. 138 (2015) 298–304. https://doi.org/10.1016/j.fuproc.2015.06.013.

[34] H. Hwang, O. Sahin, J.W. Choi, Manufacturing a super-active carbon using fast pyrolysis char from biomass and correlation study on structural features and phenol adsorption, RSC Adv. 7 (2017) 42192–42202. https://doi.org/10.1039/c7ra06910c.

[35] A.T. Tag, G. Duman, S. Ucar, J. Yanik, Effects of feedstock type and pyrolysis temperature on potential applications of biochar, J. Anal. Appl. Pyrolysis. 120 (2016) 200–206. https://doi.org/10.1016/j.jaap.2016.05.006.

[36] P. Fu, W. Yi, X. Bai, Z. Li, S. Hu, J. Xiang, Effect of temperature on gas composition and char structural features of pyrolyzed agricultural residues, Bioresour. Technol. 102 (2011) 8211–8219. https://doi.org/10.1016/j.biortech.2011.05.083.

[37] R.K. Sharma, J.B. Wooten, V.L. Baliga, X. Lin, W.G. Chan, M.R. Hajaligol, Characterization of chars from pyrolysis of lignin, Fuel. 83 (2004) 1469–1482. https://doi.org/10.1016/j.fuel.2003.11.015.

[38] A. Budai, L. Wang, M. Gronli, L.T. Strand, M.J. Antal, S. Abiven, A. Dieguez-Alonso, A. Anca-Couce, D.P. Rasse, Surface properties and chemical composition of corncob and miscanthus biochars: Effects of production temperature and method, J. Agric. Food Chem. 62 (2014) 3791–3799. https://doi.org/10.1021/jf501139f.

[39] J.A. Ippolito, L. Cui, M.G. Johnson, Biochar for Mine-land Reclamation, Biochar from Biomass Waste. (2019) 75–90. https://doi.org/10.1016/B978-0-12-811729-3.00005-4.

[40] X. Zhang, H. Wang, L. He, K. Lu, A. Sarmah, J. Li, N.S. Bolan, J. Pei, H. Huang, Using biochar for remediation of soils contaminated with heavy metals and organic pollutants., Environ. Sci. Pollut. Res. Int. 20 (2013) 8472–8483. https://doi.org/10.1007/s11356-013-1659-0.

[41] K. Lou, A.U. Rajapaksha, Y.S. Ok, S.X. Chang, Pyrolysis temperature and steam activation effects on sorption of phosphate on pine sawdust biochars in aqueous solutions, Chem. Speciat. Bioavailab. 28 (2016) 42–50. https://doi.org/10.1080/09542299.2016.1165080.

[42] S. Nanda, P. Mohanty, K.K. Pant, S. Naik, J.A. Kozinski, A.K. Dalai, Characterization of North American Lignocellulosic Biomass and Biochars in Terms of their Candidacy for Alternate Renewable Fuels, Bioenergy Res. 6 (2013) 663–677. https://doi.org/10.1007/s12155-012-9281-4.

[43] B. Chen, D. Zhou, L. Zhu, Transitional adsorption and partition of nonpolar and polar aromatic contaminants by biochars of pine needles with different pyrolytic temperatures, Environ. Sci. Technol. 42 (2008) 5137–5143. https://doi.org/10.1021/es8002684.

[44] X. Li, Q. Shen, D. Zhang, X. Mei, W. Ran, Y. Xu, G. Yu, Functional Groups Determine Biochar Properties (pH and EC) as Studied by Two-Dimensional 13C NMR Correlation Spectroscopy, PLoS One. 8 (2013). https://doi.org/10.1371/journal.pone.0065949.

[45] P. Mohanty, S. Nanda, K.K. Pant, S. Naik, J.A. Kozinski, A.K. Dalai, Evaluation of the physiochemical development of biochars obtained from pyrolysis of wheat straw, timothy grass and pinewood: Effects of heating rate, J. Anal. Appl. Pyrolysis. 104 (2013) 485–493. https://doi.org/10.1016/j.jaap.2013.05.022.

[46] D. Himmelsbach, S. Khalili, D. Akin, The use of FT-IR microspectroscopic mapping to study the effects of enzymatic retting of flax Linum usitatissimum L stems, J. Sci. Food Agric. 82 (2002) 685–696. https://doi.org/10.1002/jsfa.1090.

[47] H. Li, X. Dong, E.B. da Silva, L.M. de Oliveira, Y. Chen, L.Q. Ma, Mechanisms of metal sorption by biochars: Biochar characteristics and modifications, Chemosphere. 178 (2017) 466–478. https://doi.org/10.1016/j.chemosphere.2017.03.072.

[48] J. Sun, F. Lian, Z. Liu, L. Zhu, Z. Song, Biochars derived from various crop straws: Characterization and Cd(II) removal potential, Ecotoxicol. Environ. Saf. 106 (2014) 226–231. https://doi.org/10.1016/J.ECOENV.2014.04.042.